Int J Adv Manuf Technol (2002) 20:741–748

The International Journal of
Advanced
Manufacturing
Technology

Machining Tactics for Interior Corners of Pockets

H. S. Choy and K. W. Chan

Department of Mechanical Engineering, The University of Hong Kong, Pokfulam Road, Hong Kong

The cutter–workpiece contact of an end mill fluctuates when cutting along a curvilinear tool path. It increases sharply when reaching a concave corner. Since conventional contour-parallel tool-path cutting does not take this condition into account, it will cause a momentarily rise of cutting resistance in concave corner regions, producing undesirable effects such as machine chatter, gouging and even cutter breakage.

This paper proposes to use machining tactics in which a corner-looping tool path is employed to remove progressively the concentrated material at corner regions, thereby restricting the cutting resistance to an acceptable level. Different corner types are categorised and the procedures of generating the proposed machining tactics are described. Experimental results demonstrate that using the proposed machining tactics can significantly control and reduce the cutting resistance fluctuation encountered in concave corner regions.

Keywords: CAD/CAM; Machining tactics; Pocket; Tool path

1. Introduction

A popular mechanical operation used for forming a cavity in a workpiece is pocket milling. Numerically controlled (NC) tool paths so far developed commonly used for clearing away the material inside a pocket can be classified into two major types, namely linear and nonlinear. Examples of simple and easy-to-generate linear tool paths are the zig and the zigzag tool paths as shown in Figs 1(*a*) and 1(*b*). The zig path is a uni-directional cutting path, and hence a consistent up-cutting or down-cutting chip removal method can be maintained. However, as the cutter must be returned to the start-cut position at the end of each cutting path, there is a considerable amount of non-productive time involved. In contrast, the zigzag path is a bidirectional cutting path in which material is removed both in the forward and backward paths. Although the zigzag tool path can reduce non-productive tool positioning time, it has the disadvantage that up-cut and down-cut methods are alternately applied. This leads to problems such as machine chatter and shorter tool life.

An example of a nonlinear tool path is the contour-parallel tool path shown in Fig. 1(*c*), this tool-path pattern is derived from the boundary of the machining region concerned. It is in the form of a number of horizontal layers of contour lines which are formed by repeatedly offsetting the pocket boundary inwards with a stepover. It is a coherent tool path in the sense that the cutter is kept in contact with the cutting material for most of the time, so it incurs less idle time such as time spent in lifting, positioning and plunging the cutter. At the same time, it can also maintain the consistent use of either the up-cut or down-cut method throughout the cutting process. The contour-parallel tool path is therefore widely used as a cutting tool path, especially for large-scale material removal inside a cutting region.

The contour-parallel tool-path generation can be divided into the "intersection" approach [1,2] and the "Voronoi diagram" approach [3]. It is often required to extend and trim the offset curve segments during the contour generation process. Whichever approach is used for tool-path generation, offset contours are usually comprised of concave and convex corners that are formed by the intersection of different types of geometric entities such as lines and arcs.

The cutting problem produced by these corners has not been addressed sufficiently as it is observed that the contour-parallel tool path generated by most contemporary CAM systems will produce a small amount of uncut material at corner regions when the stepover is greater than cutter radius, as illustrated

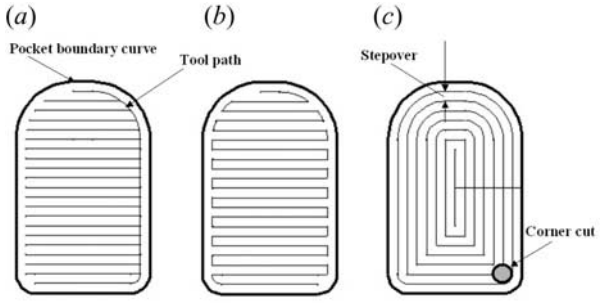

Fig. 1. Three commonly used tool paths. (*a*) Zig cut. (*b*) Zigzag cut. (*c*) Contour-parallel cut.

Correspondence and offprint requests to: Dr H. S. Choy, Department of Mechanical Engineering, The University of Hong Kong, Pokfulam Road, Hong Kong. E-mail: hangshan@hkem.com

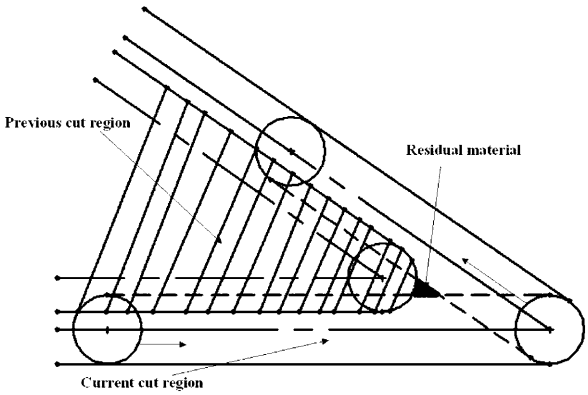

Fig. 2. Residual material left for 0.75D stepover.

in Fig. 2. Some CAM systems attempt to eliminate the amount of residual material at corner positions by appending a tusk path as shown in Fig. 3. However, driving a cutter along the tusk path is equivalent to executing a slot-cutting operation during which the cutter will be subject to up-cutting force on one side and down-cutting force on the other side. This is undesirable especially in high-speed milling applications as it will produce severe cutting-force jerk, rapid tool wear and even tool breakage.

One approach to avoid this sudden rise of cutting resistance at a corner region is to adjust the feedrate so as to limit the cutting force induced on the cutting tool [4–6]. However, using tool-path trajectories with variable feedrates requires sophisticated NC machines whose controllers can respond fast enough to the rapid change of cutting feedrates. Another approach is to modify the tool-path geometry. This approach is particularly suitable for high speed machining [7–9] as a more stable cutting load can be achieved. The governing equations of the cutter engaged angle for different cutting segments shown in Fig. 4 are:

$$\text{Linear cutting} \quad \cos(\Theta) = 1 - s/r \tag{1}$$

$$\text{Concave arc cutting} \quad \cos(\Theta) = 1 - s/r - \Pi \tag{2}$$

$$\text{Convex arc cutting} \quad \cos(\Theta) = 1 - s/r + \Pi \tag{3}$$

where $\Pi = s\ (r - 0.5s)\ /\ (Rr)$ and τ, s, r and R are the engaged angle, radial depth of cut, cutter radius and circular cutting path radius, respectively. $\Pi \geqslant 0$ since $2r \geqslant s$. Also, Θ decreases as s decreases, the cutter engaged angle can therefore be controlled by adjusting the radial depth of cut. It should be noted that if the engaged angles for line, concave, and convex arc cuts for a given stepover distance are φ, ω, and δ, respectively, the descending order of magnitudes for these angles is $\omega > \varphi > \delta$. Iwabe et al. [10] studied the increase of cutter contact angle during corner cutting and presented a looping tool path for removing the accumulated material at inside corners. Tsai et al. [11] later reported the use of an improved version of Iwabe's corner looping tool path. However, both Iwabe and Tsai's methods can only deal with simple inside corners that are formed by the intersection of line segments.

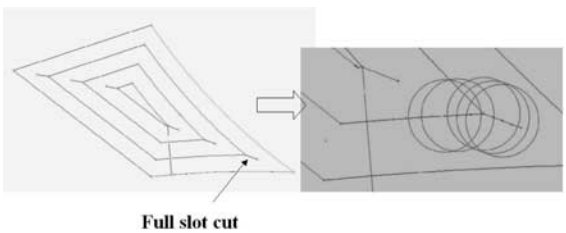

Fig. 3. The corner cutting method found in some CAD systems.

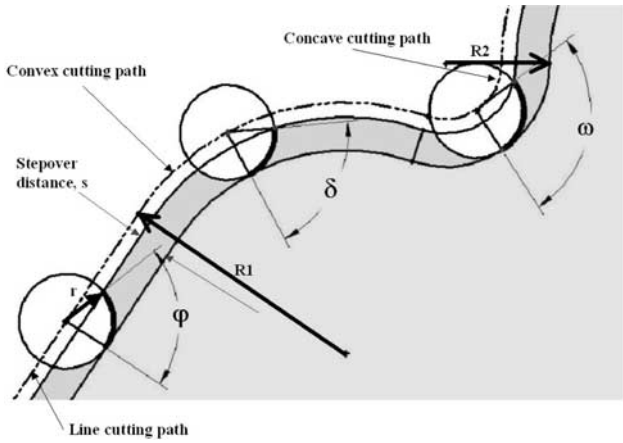

Fig. 4. Cutter engaged angles.

In view of this corner-cutting problem, Iwabe's corner looping tool-path method and its ability are adopted and extended to deal with more complicated corner shapes formed by different combinations of line and arc segments.

The rest of this paper is structured in the following manner. Section 2 categorises the types of tool path and corners. Section 3 summarises the algorithm for generating the tool path of the proposed machining tactics. In Sections 4 and 5, construction procedure and criterion of these tactics at corners is explained and defined, respectively. In Section 6, the implementation of the method is presented and the use of cutting experiments to verify the effect of the proposed method is described. Furthermore, the cutting results are discussed and examples are given to demonstrate the usefulness of the proposed machining tactics at corners. Section 7 concludes this work.

2. Category of Tool Path and Corner Shapes

Only three types of entities: line, clockwise (CW) arc and anti-clockwise (ACW) arc as shown in Figure 5 are considered in contour-parallel tool path milling patterns. A CW arc and an ACW arc are defined as follows. Imagine an arc lying on a 2D plane and with a starting point a and an ending point b.

Fig. 5. Tool-path geometries.

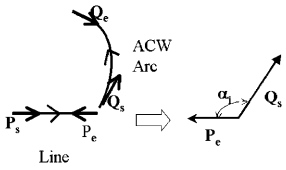

Fig. 6. Tangent vectors of two consecutive segments.

By applying the righthand screw rule, if the thumb points outward from the 2D plane when the fingers point from *a* to *b* along the arc, then the arc is an ACW arc. If the thumb points into the 2D plane, then the arc is a CW arc.

A concave and a convex corner are also defined as follows. Suppose the included angle between two tangent vectors of two connected segments shown in Fig. 6 is α_i. If $\alpha_i \geqslant \pi$, then the corner is convex, else if $\alpha_i < \pi$, then the corner is concave. Only concave corners are considered in this work.

By considering the traversal order and the geometry types of two connected segments, nine types of concave corners can be defined, as shown in Fig. 7. Based on these nine types of corner, two machining tactics were formulated:

1. Single-loop strategy (SLS).
2. Double-loop strategy (DLS).

They are presented in the following sections.

3. Tool Path Generation for the Proposed Machining Tactics

An algorithm for generating the proposed tool path for the two machining tactics is summarised as follows:

Contour-parallel tool-path generation

1. For a given $2\frac{1}{2}$ D pocket, generate a conventional contour-parallel tool path for a z-level of cut.

Sorting and labelling of contour segments

2. Sort the contour segments in a sequential order starting from the innermost point of the contour and label the geometry type of each segment. For a line segment, it will be tagged as (Line, x_1, y_1, x_2, y_2), where (x_1, y_1) and (x_2, y_2) are the coordinates of the starting and ending points respectively. Similarly, for ACW and CW arcs, the labels will be (ACW arc, x_1, y_1, x_2, y_2, xc, yc, r) and (CW arc, x_1, y_1, x_2, y_2, xc, yc, r) respectively, where (xc, yc) and r are the centre coordinates and radius of the arc, respectively. The labelled contour segments are stored in a linked list structure.

Identification of a concave corner

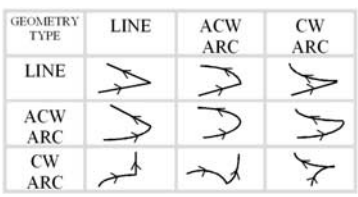

Fig. 7. Different corner types.

3. For two consecutive segments in the linked list structure, say *P* and *Q*, determine whether they form a concave corner according to the previously described definition. If they form a concave corner, go to step 4. Otherwise, consider the next consecutive segment pair starting with segment *Q*.

Calculation of the tool path of the proposed machining tactic depending on corner type

4. Evaluate the corner type according to the geometry previously labelled in step 2. Calculate the tool path for the corner concerned based on the method described in Section 4. The appended tool path is then labelled and inserted in the linked list structure. Return to step 3 for the remaining consecutive segments. After calculating the appended tool path for all concave corners, go to step 5.

Generation of cutter location file

5. Traverse the linked list structure again and generate a cutter location coordinates file based on the geometric information appended in each contour segment.

4. Construction Procedure

Consider a corner formed by two straight line segments as shown in Fig. 8. The current cutter paths are two straight lines, *U* and *V*, while the previous cutter paths are lines *PU* and *PV*. Their equations are governed by

$$\text{Line } U: \quad ax + by + d + kt_1 = 0 \tag{4}$$

$$\text{Line } V: \quad Ax + By + D + Kt_1 = 0 \tag{5}$$

$$\text{Line } PU: \quad ax + by + d + k(t_1 + s) = 0 \tag{6}$$

$$\text{Line } PV: \quad Ax + By + D + K(t_1 + s) = 0 \tag{7}$$

where *a, b, A, B, d, D* are coefficients, *k* and *K* represents offset direction, t_1 is the offset distance of lines *U* and *V* from the given pocket boundary and *s* is the stepover distance of lines *PU* and *PV* from lines *U* and *V*.

As described by Persson [3], the corner bisector for this line-line corner type is a line bisector. The parametric equations that govern this line bisector are:

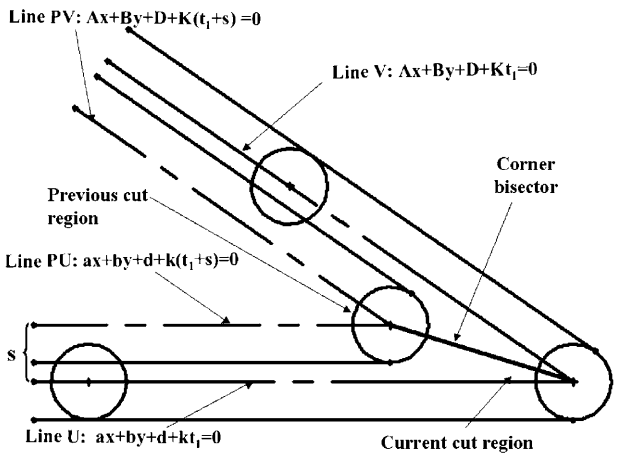

Fig. 8. Conventional corner tool paths.

$$x(t) = (bD - Bd)/N + t(bK - Bk)/N \quad (8)$$

$$y(t) = (Ad - aD)/N + t(Ak - aK)/N \quad (9)$$

$$N = aB - bA \quad (10)$$

where t is a parameter, $t_1 < t < t_1 + s$.

4.1 Single-Loop Strategy (SLS)

Considering a pocket to be an area removed by using a contour-parallel tool path, the cutter is assumed to start from the innermost point of the contour tool path and cut outwards along the contour tool path. A portion of a concave corner of the contour tool path is shown in Fig. 9. The contour tool path represents the loci of the cutter centre. For explanation purposes, the corner is assumed to be formed by two linear contour segments *ABC* and *DEF*. Segment *ABC* is the current tool path under consideration whereas segment *DEF* is the previous trace of tool path. A corner bisector is constructed at the concave corner as shown. The corner bisector is defined as the locus of points which are equidistant from the two adjacent curve segments of the concave corner. The length of the corner bisector is defined by the intersection points formed between the corner bisector and contour segments *ABC* and *DEF*. The midpoint *H* of the corner bisector is also determined.

In SLS, the cutter is driven along the current contour tool-path segment *ABC*. When the cutter reaches point *G*, the cutter follows the arc *GHI,* passing through midpoint *H* and rejoining segment *ABC* again at point *I*. The cutter then moves back from point *I* to point *G* again through the straight line path *IG*. The cutter finally completes the corner cut by moving from point *G* to points *B* and *C*. The idea of SLS is to separate the removal of the corner material into two portions so that the level of cutting load can be reduced.

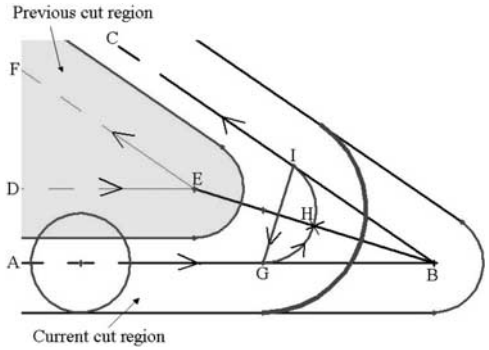

Fig. 9. Single-loop strategy (SLS).

There are two steps in the construction of SLS (Fig. 10). They are as follows:

Step 1. Finding points *H* and *M* on the corner bisector
Lines *U* and *V* are offset inwards by an amount equal to *s*/2. The offset lines intersect at point *M* which is also a point on the corner bisector. Point *H* is the intersection of lines *PU* and *PV*.

Step 2. Arc fitting.
Fit a circular arc to pass through point *M* such that the circular arc satisfies

$$x = r\cos(\phi) + m \quad (11)$$

$$y = r\sin(\phi) + n \quad (12)$$

$$(x - m)^2 + (y - n)^2 = r^2 \quad (13)$$

where (m, n) are the coordinates of the centre-point, *CP*, and r is the radius of the circular arc, respectively, ϕ is an angle for the circular arc to sweep from starting angle to ending angle. This arc is the required corner loop.

A bisection-like algorithm is used to determine the values of m and n. The procedure for this algorithm is summarised in the following four steps:
A function $Z(\Psi) = \text{Dist}(\Psi, M) - r$ is first defined where Ψ is a point with coordinates (Ψ_x, Ψ_y), r is a radius equal to the normal distance between the point Ψ and lines *U* or *V*, and Dist (,) is an operator representing the distance between two points.

1. Find two points P_L and P_U with coordinates (m_L, n_L) and (m_U, n_U), respectively, such that $r_U > r_L$ and $Z(P_L) < 0$ and $Z(P_U) > 0$.

2. For the two intervals between m_L and m_U and between n_L and n_U, find a new midpoint *MM* with coordinates $((m_L+m_U)/2, (n_L+n_U)/2))$.

3. If $Z(MM) = 0$ then *MM* is a point with the same coordinates (m, n) as *CP*, else if $Z(MM) < 0$ then let m_L and $n_L = x$ and y coordinates of *MM*, respectively, else if $Z(MM) > 0$ then m_U and $n_U = x$ and y coordinates of MM.

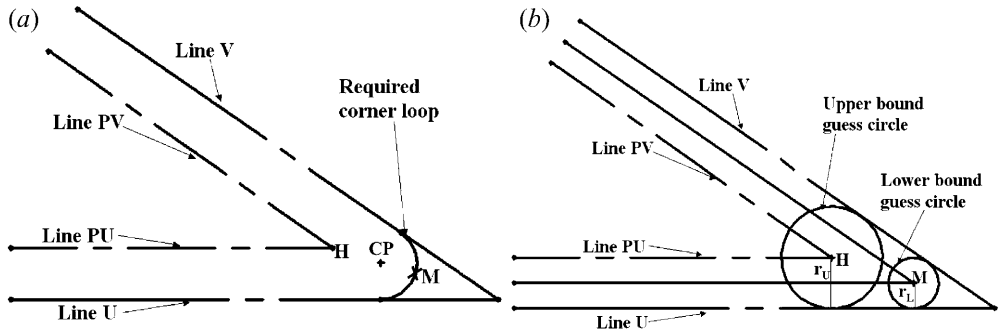

Fig. 10. SLS corner-looping construction. (*a*) Corner loop construction in SLS. (*b*) Bisection-like method.

4. Repeat steps 2 and 3 until $Z(MM_i) = 0$ or $|Z(MM_i)| <= \text{DOA}$, where || is a magnitude operator and DOA stands for a defined degree of accuracy.

Estimation of initial points for P_L and P_U.

The points M and H are chosen as the points P_L and P_U, respectively. For point M, it satisfies $Z(M) = -r_L < 0$. Point H is determined by considering the following cases:

Case 1. Dist $(H,M) < r_U$, the offset distance s will be increased incrementally by an amount $s/2$ until Dist $(H,M) \geqslant r_U$. If Dist $(H,M) > r_U$ then point H becomes point P_U, else go to Case 2.

Case 2. Dist $(H,M) = r_U$, it means that the coordinates (m_U, n_U) of point H are the exact values for m and n respectively and the above numerical iteration procedure will terminate.

Case 3. Dist $(H,M) > r_U$, point H becomes point P_U.

After several iterations with a DOA set to 10^{-3}, point MM_i is determined. Its x and y coordinates approach to the values of m and n, respectively. The normal distance between point MM_i and line U (or line V) is the radius of the required corner loop which passes through point M.

4.2. Double-Loop Strategy (DLS)

DLS aims to further reduce the level of cutting force encountered at the corner by dividing the total material to be removed into three portions. This is done by constructing two cutting loops. As shown in Fig. 11, points H and K divide the length of the corner bisector into $\frac{2}{3}$ and $\frac{1}{3}$, respectively. In the first cutting loop, the cutter centre passes through points *AGHIG*. In the second loop, the cutter centre passes through points *JKLJ*. The cutter centre then moves through points *BLIC* to remove the material in the corner.

In comparing with SLS, DLS consists of two individual single loop constructions (Fig. 12). Their P_U points can be found with the same method as above. However, their P_L points are different and their determination is explained as follows. For the first single loop construction, lines U and V are offset an amount equal to $(2s)/3$ to determine point M. In this way, point M is no longer the mid-point of the corner bisector; instead, it is a point such that $HM/HG = \frac{1}{3}$. For the second loop construction in DLS, lines U and V are offset by an amount equal to $s/3$ to determine point M. Point M now becomes a point such that $HM/HG = \frac{2}{3}$.

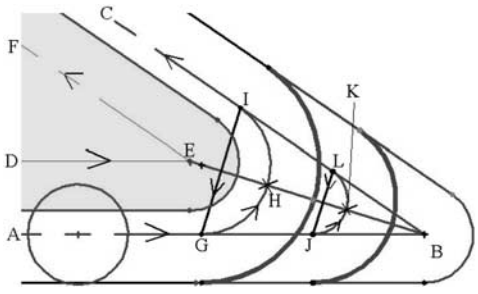

Fig. 11. Double-loop strategy (DLS).

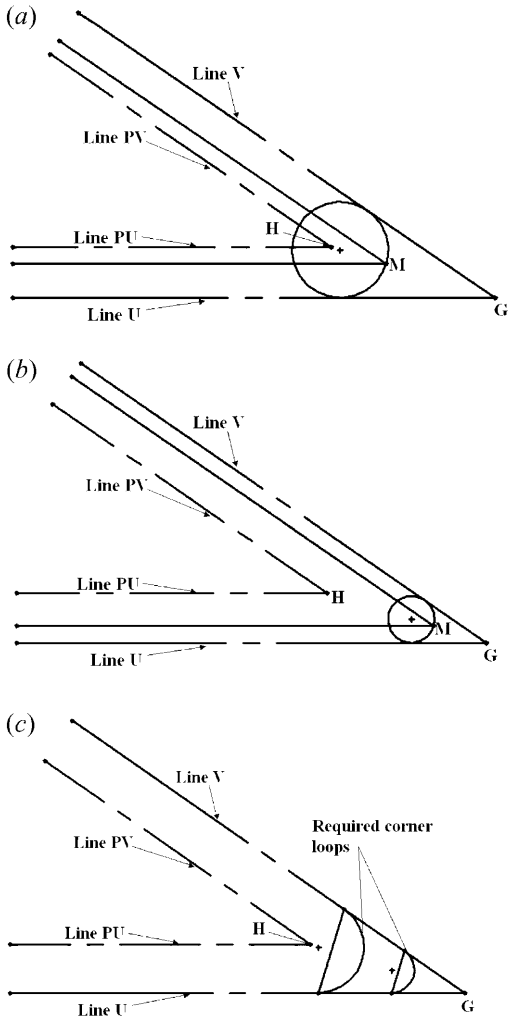

Fig. 12. The DLS construction procedure. (*a*) First corner loop construction in DLS. (*b*) Second corner loop construction in DLS. (*c*) Resultant corner loops in DLS.

5. Criterion for Number of Corner Loops

The determination of the number of corner loops is based on *RD* where *RD* is the ratio between corner bisector length to the cutter diameter. In most cases, SLS or DLS is enough to keep the radial depth of cut at the corner within a desired value. For some sharp corners, it may be necessary to use more corner loops in order to have a further reduction in radial depth of cut and to ensure that no material is left behind. The criterion for selecting the number of corner loops at a corner is based on the following formula:

Number of corner loops = Int(*RD*/*E*) where Int() is an integer operator, E is a reduction factor determined by the ratio of the user's desired radial depth of cut to the cutter diameter. The range of E is between 0 and 1.

6. Discussion

The SLS and DLS tool-path generation procedures were implemented as an add-on user function in the Unigraphics (UG) version 17.0 CADCAM system. The add-on program was coded in the C language within the Windows NT 4.0 operating environment and facilitated by using the UG/Open API functions.

For the experiments, a Kistler model 9257B 3-axis quartz dynamometer was used for measuring the cutting forces along the x, y, and z components. A PC installed with an A/D circuit board was used to collect the electrical voltage signals. The sampling rate was about 1 kHz/channel. A 10 mm diameter end mill was used to carry out corner cutting on mild steel using conventional contour-parallel cutting, SLS and DLS tool paths. The resultant cutting force was estimated by the following formula: resultant cutting force, $F = \sqrt{(F_x^2 + F_y^2 + F_z^2)}$ where F_x, F_y and F_z are the forces acting along the x, y and z directions, respectively.

The cutting tests proved that using the SLS and DLS pocket milling tool paths can significantly reduce the cutting force produced in a cutter when clearing corner material. As an example, the cutting test of a corner formed by ACW and CW arc segments is discussed here. Figures 13(a), 13(b) and 13(c) show the measured cutting force when cutting a corner using a conventional contour-parallel tool path, SLS tool path, and DLS tool path, respectively.

The cutting parameter settings for the three situations were the same: spindle speed = 800 r.p.m.; feedrate = 100 mm min^{-1}; axial depth of cut = 0.1 mm; and stepover = 7.5 mm. Clearly, the force pattern shown in Fig. 13(a) is different from those shown in Figs 13(b) and 13(c). This is because when using the conventional contour-parallel tool path, the cutter is effectively performing a slot-cutting action at the corner position, so there is a sudden rise in cutting force, and at that instant the cutter is subject to both up-cut and down-cut forces. Figures 13(b) and 13(c) reveal that the cutting force is lowered owing to the reduction of the radial depth of cut. Also, the cutter is consistently subject to down-cut force only. This can also be explained as follows. The total amount of material at the concerned corner is fixed. Thus, the total amount of mechanical work done to remove the material, by using the tool paths for conventional contour-parallel, SLS, and DLS cuts should be the same. However, instead of removing all the material in one pass, one or two looping passes are appended at the corner so as to remove the corner material progressively.

Besides the experimental results, two examples are demonstrated to show the effectiveness of the proposed machining tactics at corners.

Example 1 (Fig. 14) shows an application of DLS in line-line, line-ACW arc, line-CW arc corners. In this example, two looping cut tool paths at the corners concerned are mathematically appended. Example 2 (Fig. 15) shows the tool path by conventional contour-parallel cutting, SLS, and DLS of a pocket area. In comparison, the proposed SLS and DLS can be used to overcome the problems of the conventional tool-path generation at corners such that slot-cutting situation can be entirely avoided. Further experimental results prove that a more stable machining state is achieved by using the proposed machining tactics. In the experiment, feedrate was kept constant regardless of the geometry of the tool path. Cutting force was found to be well within the cutter manufacturer's recommended limit.

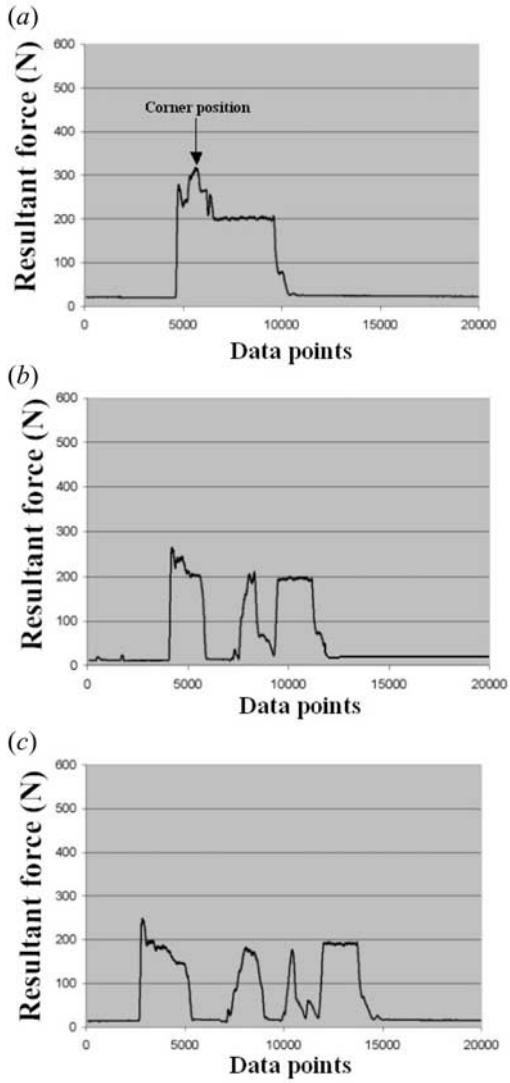

Fig. 13. The cutting force at corners. (a) Corner cut without loop. (b) Corner cut with single loop. (c) Corner cut with double loops.

7. Conclusion

In this paper, the problem of material concentration at pocket corners was addressed. Machining tactics for pocket corners were introduced. The working principle of the tactics is to remove the corner material progressively by using a single or double looping cutting motion. Cutting tests were conducted, and demonstrated that the machining tactics are useful for clearing accumulated material at pocket corners since the

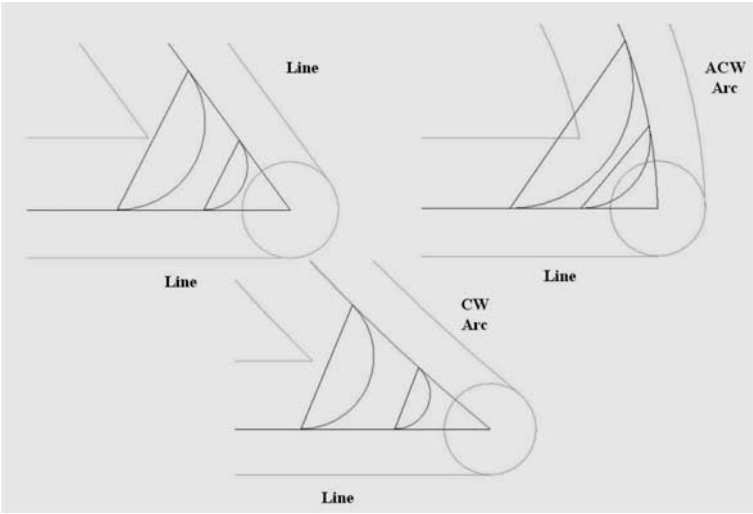

Fig. 14. Example 1 of a corner formed by line and arc.

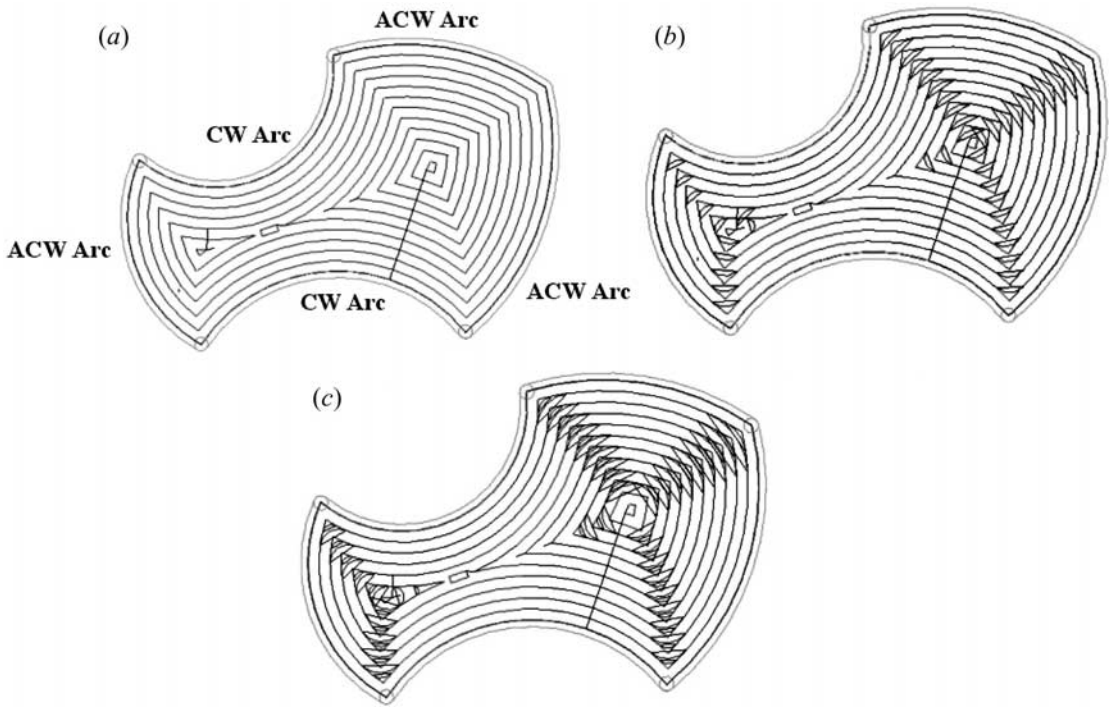

Fig. 15. Example 2 of a pocket composed of arcs. (*a*) Conventional tool path. (*b*) Single-loop tool path. (*c*) Double-loop tool path.

momentary increase in cutting force level at the corner can be suppressed by increasing the number of corner cutting loops.

References

1. A. Hansen and F. Arbab, "An algorithm for generation NC tool paths for arbitrarily shaped pockets with islands", ACM Transaction on Graphics, 11(2), pp. 152–182, 1992.
2. K. Preiss, "Automated mill pocketing computations", in Proceedings of the International Symposium on Advanced Geometric Modeling for Engineering Applications, Berlin, Germany, 1989.
3. H. Persson, "NC machining of arbitrarily shaped pockets", Computer-Aided Design, 10(3), pp. 169–174, 1978.
4. A. Spence and Y. Altintas, "CAD assisted adaptive control for milling", ASME Journal of Dynamics Systems, Measurement, and Control, 113, pp. 444–450, 1991.
5. K. Yamazaki, N. Kojima, C. Sakamoto and T. Saito, "Real-time model reference adaptive control of 3-D sculptured surface machining", Annals CIRP, 40(1), pp. 479–482, 1991.
6. W. P. Wang, "Application of solid modeling to automate machining parameters for complex parts", 19th CIRP International Seminar on Manufacturing Systems, pp. 33–37, 1987.
7. J. Tlusty and S. Smith, "Update on high-speed milling dynamics",

ASME Journal of Engineering for Industry, 112, pp. 142–149, May 1990.
8. J. Tlusty and S. Smith, "Current trends in high speed machining", Journal of Manufacturing Science and Engineering, 119(4B), pp. 664–666, November 1997.
9. W. R. Winfough and S. Smith, "Automatic selection of the optimum metal removal conditions for high speed milling", Transactions NAMRI, 23, pp. 163–166, 1995.
10. H. Iwabe, Y. Fujii, K. Saito and T. Kisinami, "Study on corner cut by end mill analysis of cutting mechanism and new cutting method at inside corner", (in Japanese), Journal of Japan Society of Precision Engineering, 55(5), pp. 841–846, 1989.
11. M. D. Tsai, S. Takata, M. Inui, F. Kimura and T. Sata, "Operation planning based on cutting process models", Annals CIRP, 40(1), pp. 95–98, 1991.